Carcinogenesis vol.34 no.9 pp.2090–2098, 2013
doi:10.1093/carcin/bgt170
Advance Access publication May 20, 2013

Sulindac inhibits pancreatic carcinogenesis in *LSL-Kras^{G12D}-LSL-Trp53^{R172H}-Pdx-1-Cre* mice via suppressing aldo-keto reductase family 1B10 (AKR1B10)

Haonan Li[†], Allison L.Yang[†], Yeon Tae Chung, Wanying Zhang, Jie Liao and Guang-Yu Yang*

Department of Pathology, Northwestern University Feinberg School of Medicine, 303 East Chicago Avenue, Ward 6-118, Chicago, IL 60611

*To whom correspondence should be addressed. Tel: +312 503 0645; Fax: +312 503 0647;
Email: g-yang@northwestern.edu

Sulindac has been identified as a competitive inhibitor of aldo-keto reductase 1B10 (AKR1B10), an enzyme that plays a key role in carcinogenesis. AKR1B10 is overexpressed in pancreatic ductal adenocarcinoma (PDAC) and exhibits lipid substrate specificity, especially for farnesyl and geranylgeranyl. There have been no studies though showing that the inhibition of PDAC by sulindac is via inhibition of AKR1B10, particularly the metabolism of farnesyl/geranylgeranyl and Kras protein prenylation. To determine the chemopreventive effects of sulindac on pancreatic carcinogenesis, 5-week-old *LSL-Kras^{G12D}-LSL-Trp53^{R172H}-Pdx-1-Cre* mice (Pan$^{kras/p53}$ mice) were fed an AIN93M diet with or without 200 p.p.m. sulindac (n = 20/group). Kaplan–Meier survival analysis showed that average animal survival in Pan$^{kras/p53}$ mice was 143.7 ± 8.8 days, and average survival with sulindac was increased to 168.0 ± 8.8 days ($P < 0.005$). Histopathological analyses revealed that 90% of mice developed PDAC, 10% with metastasis to the liver and lymph nodes. With sulindac, the incidence of PDAC was reduced to 56% ($P < 0.01$) and only one mouse had lymph node metastasis. Immunochemical analysis showed that sulindac significantly decreased Ki-67-labeled cell proliferation and markedly reduced the expression of phosphorylated extracellular signal-regulated kinases 1 and 2 (ERK1/2), c-Raf and mitogen-activated protein kinase kinase 1 and 2. In *in vitro* experiments with PDAC cells from Pan$^{kras/p53}$ mice, sulindac exhibited dose-dependent inhibition of AKR1B10 activity. By silencing AKR1B10 expression through small interfering RNA or by sulindac treatment, these *in vitro* models showed a reduction in Kras and human DNA-J homolog 2 protein prenylation, and downregulation of phosphorylated C-raf, ERK1/2 and MEK1/2 expression. Our results demonstrate that sulindac inhibits pancreatic carcinogenesis by the inhibition of Kras protein prenylation by targeting AKR1B10.

Introduction

Sulindac is one of the most effective non-steroidal anti-inflammatory drugs (NSAIDs) for cancer chemoprevention (1–5). It is a prodrug that undergoes two major biotransformations of its sulfoxide moiety: oxidation of the inactive sulfone and reduction to the pharmacologically active sulfide. The active sulfide metabolite of sulindac is responsible for cyclooxygenase (COX) inhibition with an IC_{50} of 0.02 μM although it only accounts for <6% of total sulindac and its metabolites. The recirculation of the parent sulindac and its sulfone metabolites are much more extensive than the circulating active sulfide metabolites. All of the metabolites of sulindac exhibit anticancer activities through the induction of apoptosis and suppression of tumor cell growth, angiogenesis and metastasis, mainly via COX-independent mechanisms (6,7). The precise molecular mechanisms governing these effects are not well known.

Recent studies have shown that sulindac is a potent competitive inhibitor of aldo-keto reductase family member 1B10 (AKR1B10) with an IC_{50} of 0.35μM (8). AKR1B10 is well known to be overexpressed in human pancreatic cancer (9), hepatocellular carcinoma (10,11) and smoking-related carcinomas such as lung cancer (12–18). It exhibits more restrictive substrate specificity than most human AKRs as only farnesal, geranylgeranial, retinal and carbonyls are its specific substrates (8,19–22). The metabolism of these substrates is thought to promote carcinogenesis in several ways. First, AKR1B10 reduces farnesyl and geranylgeranyl to farnesol and geranylgeraniol, which are further phosphorylated to farnesyl and geranylgeranyl pyrophosphates. These intermediates of cholesterol synthesis are highly involved in protein prenylation; this is significant because >95% of human pancreatic cancers carry the *Kras* gene mutation (8), which requires prenylation to become active (23). Second, the active carbonyl radicals induce cell apoptosis. AKR1B10 converts highly reactive aldehydic and ketonic groups into hydroxyl groups in neoplastic cells, thus preventing these neoplastic cells from undergoing carbonyl-induced apoptosis. Third, AKR1B10 is an efficient retinal reductase (19,22,24,25); it facilitates the conversion of retinal to retinol, and suppresses its conversion to retinoic acid, a major active antineoplastic metabolite. In light of the significant role of AKR1B10 in carcinogenesis, the anticancer effects of inhibiting AKR1B10 with sulindac warrant further investigation.

There has been tremendous progress in engineering mouse models of pancreatic adenocarcinomas (26,27) to not only display similar genetic alterations to those seen in humans but also identical pancreatic ductal adenocarcinomas. Using lox-p Cre technology, the *Lox-STOP-Lox(LSL)* construct is inserted into the mouse genomic *Kras* or *p53* locus, which is already engineered to have a G-A transition at codon 12 for Kras and an arg-to-his substitution at amino acid 172 for p53 (28–30). To mimic pancreatic carcinogenesis with multiple genetic alterations, triple transgenic *K-ras^{G12D}-p53^{R172H}-Pdx-1-Cre* mice (Pan$^{kras/p53}$ mice) are produced by cross-breeding Pdx-1-Cre mice with *LSL-Kras^{G12D}* mice and *LSL-Trp53^{R172H}* mice (30). These triple transgenic Pan$^{kras/p53}$ mice show concurrent activation of transgenic mutant *K-ras^{G12D}* and *p53^{R172H}* genes in the Pdx-1+ pancreatic epithelial cells recombinated by Pdx-1-cre, develop pancreatic ductal adenocarcinomas (PDAC) and have an average survival of 5–6 months (30). This unique genetically engineered mouse model of pancreatic cancer most closely mimics the genetic alterations seen in humans and also has PDACs most identical to those seen in humans with features of moderate–poorly differentiated PDAC and metastasis to the liver and lymph nodes (31).

In the present studies, the inhibitory effects and mechanism of sulindac on pancreatic carcinogenesis were systematically investigated in Pan$^{kras/p53}$ mice. Animal survival and the development of PDAC and its metastasis were used as the endpoint markers to evaluate chemopreventive effects. Immunohistochemistry was used to analyze cell proliferation and Kras-activated phosphorylated extracellular signal-regulated kinases 1 and 2 (ERK1/2), c-Raf and mitogen-activated protein kinase kinase 1 and 2 (MEK1/2) signals, as well as the expression levels of AKR1B10 and COX2. The specific effects of sulindac on AKR1B10 enzyme activity and expression as well as AKR1B10-modulated protein prenylation, particularly in inhibiting Kras and nuclear HDJ2 protein prenylation and Kras downstream signals, were determined in a mouse PDAC cell line P03 derived from Pan$^{kras/p53}$ mice and compared with a P03 cell line with small interfering RNA (siRNA) silencing of AKR1B10.

Abbreviations: AKR1B10, aldo-keto reductase 1B10; COX, cyclooxygenase; c-Raf, RAF proto-oncogene serine/threonine–protein kinase; DMEM, Dulbecco's modified Eagle's medium; ERK1/2, extracellular signal-regulated kinases 1 and 2; HDJ, human DNA-J homolog; MEK1/2, mitogen-activated protein kinase kinase 1 and 2; NSAID, non-steroidal anti-inflammatory drugs; PDAC, pancreatic ductal adenocarcinoma; siRNA, small interfering RNA.

[†]These authors contributed equally to this work.

Materials and methods

Animals

Pdx-1-Cre mice were kindly provided by Dr Lowy (University of Cincinnati). LSL-*Trp53*^{R172H} and LSL-*Kras*^{G12D} mice were obtained from Mouse Models of Human Cancers Consortium, National Cancer Institute/National Institutes of Health and kindly provided by Dr T.Jacks (Massachusetts Institute of Technology). All mice were genotyped in our laboratory following the protocols provided by the investigators (30). To produce triple transgenic *Kras*^{G12D}-*Trp53*^{R172}-*Pdx-1-Cre* mice (called Pan$^{kras/p53}$ mice), double transgenic LSL-*Kras*$^{G12D/+}$-LSL-*Trp53*$^{R172/+}$ mice were first generated by cross-mating LSL-*Trp53*^{R172H} and LSL-*Kras*^{G12D} mice, and then LSL-*Kras*$^{G12D/+}$-LSL-*Trp53*$^{R172/+}$ mice were further mated with transgenic *Pdx-1-Cre* mice. Mice were housed under pathogen-free conditions in the facilities of Laboratory Animal Services, Northwestern University. All studies were conducted in compliance with Northwestern University IACUC guidelines.

Animal experiments

Five-week-old Pan$^{kras/p53}$ mice were fed an AIN93M diet or an AIN93M diet supplemented with 200 p.p.m. sulindac throughout the experiment period (n = 20 mice per group, both genders, 10 mice per gender per group). The selection of 200 p.p.m. sulindac is based on the more appropriate conversion of drug doses from animal studies to humans (32). Sulindac was purchased from Sigma (St Louis, MO). The AIN93M diet was purchased from Research Diets (New Brunswick, NJ).

Animals were monitored daily for the development of pancreatic carcinoma with the markers being abdominal distension (due to production of malignant ascites) and weight loss (>20%). Animals with these signs were generally in the late stages of pancreatic carcinoma, and thus were killed immediately and recorded for the survival from the pancreatic cancer. When the accumulated mortality reached 75% in a group or reached a statistical significance, the animal experiment was terminated and all remaining mice were killed.

Tissue preparation and histopathology

The mice were killed by CO_2 asphyxiation. Pancreases and other organs including liver, spleen, adrenals, kidney and lung were collected. The numbers and sizes of tumors were recorded, and three perpendicular diameter measurements were obtained for each tumor using calipers. Tumor volume was determined by the equation $V = 4/3\pi r^3$, where r was the average tumor radius obtained from the three diameter measurements. The organs were fixed in 10% formalin for 24 h, routinely processed and embedded in paraffin. Serial paraffin sections (5 μm) were made and stained with hematoxylin and eosin for histopathological examination. Additional tissue sections were obtained on poly-L-lysine-coated slides for immunohistochemical analyses.

Pancreatic tumors were analyzed histopathologically according to the established criteria (33). The tumors were classified as PDAC with well, moderate to poorly differentiated morphology. Chronic pancreatitis and precancerous lesions were also analyzed based on previously published criteria (31,33,34).

Immunohistochemistry

Immunohistochemical staining was performed according to our routine protocol using an avidin–biotin–peroxidase method (31,35). Endogenous peroxidase activity was quenched in paraffin-embedded tissue sections with 1% H_2O_2. Antigens were retrieved using citrate buffer in a microwave. Nonspecific protein–protein interactions were blocked with diluted normal horse serum. Slides were then incubated with primary antibody (1 μg/ml for Ki-67, phosphorylated ERK1/2 or CM-5p p53 antibody), followed by the appropriate biotinylated secondary antibody and the avidin–biotin–peroxidase complex for 45 min each. Anti-Ki-67, anti-phosphorylated EEK1/2 and anti-p53 antibodies were purchased from Vector Labs (Burlingame, CA). 3,3′-Diaminobenzidine was used as the chromagen. Negative controls were established by replacing the primary antibody with phosphate-buffered saline and normal serum. Positive staining was indicated by the presence of a specific brown-colored precipitate.

Positive cells and staining intensity were quantified for all antibodies using a Olympus BX45 microscope and DP70 digital Camera. The full image of each pancreas was snapped under ×2.5 and ×20 objective lens and saved with >2560 resolution image. Using 'histogram analysis' in the Photoshop program, specific staining intensity and percentage of positive staining cell number in total cells counted were be measured for at least 10 defined area/image including normal pancreas, acinar–ductal metaplasia, PanINs and PDAC in each pancreas, and automatically expressed as mean value ± SD.

Cell culture, proliferation/colony formation assay

Cell lines were allowed to grow in a monolayer in Dulbecco's modified Eagle's medium (DMEM) culture medium with 10% fetal bovine serum. Cell proliferation and tumorigenecity were determined using the colony formation assay. The assays were used to find cell anchorage-independent growth or proliferation. Cells were mixed with sulindac or solvent (water) in 3 ml of culture medium and seeded into 6 well culture plates (each dose of agent in triplicate) with 200 cells per well. Cell proliferation was measured using a colony formation assay after 14 days. The percentage of inhibition of cell colony formation (only colonies with >50 cells were counted) was calculated as compared with the control.

AKR1B10 enzyme activity assay

Cells were lysed on ice in buffer containing 50 mM Tris-HCl (pH 7.0), 1% protease inhibitor (Sigma–Aldrich, St Louis, MO), 1% β-mercapethanol (Sigma–Aldrich), 10% RIPA buffer (Santa Cruz Biotechnology, Santa Cruz, CA) by vortexing briefly every 5 min over a 30 min period, followed by centrifugation at 10 000 r.p.m. at 4°C for 10 min. Soluble proteins in the supernatant (50 μg) were used for AKR1B10 activity assays in a reaction buffer containing of 125 mM sodium phosphate (pH 7.0), 50 mM KCl and 20 mM DL-glyceraldehyde in a 35°C water bath for 10 min. The reaction is carried out using 0.3 mM reduced nicotinamide adenine dinucleotide phosphate as a substrate for AKR1B10 enzymatic activity. The change/decrease in optical density at 340 nm is monitored every minute for 10 min at room temperature in a SmartSpec Plus spectrophotometer (Bio-Rad, Hercules, CA), and the difference in absorbance from the start to the end of the assay (10 min period) was used to determine AKR1B10 activity (9).

Cell fractionation and western blot analysis

Whole cells were lysed in complete lysis buffers (Santa Cruz Biotechnology), containing a cocktail of phosphatase, protease and proteosome inhibitors followed by centrifugation at 900g at 4°C for 20 min. The supernatants were further centrifuged at 105 000g at 4°C for 90 min. The cytosolic fractions (supernatant) were collected and kept at −80°C for further analysis. The pellets were washed and the membrane fractions were recovered by centrifugation at 105 000g at 4°C for 90 min. The membrane pellets were resuspended in 0.25M sucrose solution with a cocktail of inhibitors and stored at −80°C. The protein concentrations were determined using a bicinchoninic acid protein assay kit (Pierce, Rockford, IL). Heat-denatured membranous and cytosolic fractions underwent sodium dodecyl sulfate–polyacrylamide gel (4–12% gradient) electrophoresis. The resolved proteins were transferred onto polyvinylidene fluoride membrane and probed with the primary antibody in blocking buffer at 4°C overnight. After washing with tris-buffer three times, the membrane was incubated with secondary antibody and visualized by enhanced chemiluminesence (Amersham Kit, Arlington Heights, IL). Specific protein band intensity was quantified using Image-Pro Plus.

Active Kras pull-down assay

P03 cells were cultured in DMEM medium supplemented with 10% fetal bovine serum for 18 h, treated with sulindac at doses of 0.1, 0.4 and 0.8 mM for 24 h in DMEM 10% fetal bovine serum. Active form of Kras level was determined by an active Ras pull-down assay kit (Pierce), according to the manufacturer's instruction. Cell lysates (1 mg of total cell protein in each sample) were incubated with 10 μg Raf-1-RBD for 45 min at 4°C and centrifuged for 15 s at 14 000g to pellet the agarose beads. After discarding the supernatant, agarose beads were washed three times with 500 μl of lysis buffer, and the pellets were resuspended in 2× Laemmli sample buffer containing dithiothreitol, boiled for 5 min and centrifuged at 14 000g. The supernatant was collected and cellular proteins resolved by 12% sodium dodecyl sulfate–polyacrylamide gel electrophoresis and analyzed by western blotting using a Kras-specific antibody.

Silencing AKR1B10 expression using a small interfering RNA approach

Sense (5′-AGAGGAAUGUGAUUGUCAUTT-3′) and anti-sense (5′-AUGACAAUCACAUUCCUCUGG-3′) oligonucleotides were purchased from Ambion (Austin, TX) for ABR1B10. The oligonucleotides were annealed following the manufacturer's protocol to generate the double-stranded siRNAs at the final concentration of 20 μM. Cells (2×10^6) were cultured in six well plastic plates in 1 ml of DMEM without serum and transfected at ~40% of confluence by adding 4 μl of oligofectamine (Invitrogen) and 10 μl of 20 μM stock siRNAs. Cells were incubated at 37°C for 4 h in a CO_2 incubator, followed by the addition of growth medium containing 3× the normal concentration of serum. Cells were maintained in culture for an additional 32 h before western blot or enzyme activity analysis.

Statistical analysis

The data were expressed as mean ± SE. Statistical significance was tested using SigmaStat Version 1.01 software (Jandel Scientific, San Rafael, CA). Kaplan–Meier survival analysis with log-rank Test was performed. Tumor incidence was analyzed using the chi-square test. Normally distributed data were analyzed using Student's t-test, and non-parametric data, such as tumor multiplicity, were analyzed using the Mann–Whitney rank sum test.

Results

Sulindac increases Pan$^{kras/p53}$ mice survival

Survival of Pan$^{kras/p53}$ mice was used as the endpoint marker to evaluate the chemopreventive effect of sulindac. Mice were fed either a standard AIN93M diet or an AIN93M diet with 200 p.p.m. sulindac supplementation (treatment group). At day 160, sixteen of 21 Pan$^{kras/p53}$ mice died of pancreatic carcinoma [survival rate: 23.8% (5 of 21 mice)]. In contrast, only 6 of 19 Pan$^{kras/p53}$ mice treated with sulindac died of pancreatic carcinoma [survival rate: 68.4% (13 of 19 mice)]. At this time point, the entire experiment was terminated. Figure 1A shows the Kaplan–Meier survival analysis with log-rank test: Pan$^{kras/p53}$ mice treated with 200 p.p.m. sulindac exhibited a significant increase in animal survival as compared with mice not given sulindac (P = 0.0005). Average survival in the group given the regular AIN93M diet was 143.7 ± 8.8 days (mean ± SE, 95% lower 126.4 days and 95% upper 160.9 days) and average survival in the AIN93 plus 200 p.p.m. sulindac group was appreciably increased to 168.1 ± 8.8 days (mean ± SE, 95% lower 150.8 days and 95% upper 185.3 days).

Body weight, food and water consumption were monitored throughout the duration of the experiment; there was no difference in food or water consumption between the mice in the AIN93M group and the mice in the AIN93M plus 200 p.p.m. sulindac group. Weekly body weight measurements showed no statistical difference between the average body weights of the mice in either group (Supplementary Figure 1s, available at *Carcinogenesis* Online). All key organs from the mice were collected, weighed and examined grossly. Figure 1B–D shows the distribution of organ weights for the pancreas, liver and spleen. Of 20 mice fed the normal AIN93M diet, four had increased pancreas and liver weights and three had significant increases in spleen weight. In the sulindac-treated Pan$^{kras/p53}$ mice, only two exhibited an increase in pancreas weight, whereas the weights of the liver and spleen were below average.

Histopathological analysis was performed for all of the key organs including gastrointestinal tract, kidney, spleen, liver, lung and heart. There was no pathologic alteration or toxicity identified in these organs, particularly no ulcers, erosions or fibrosis (the representative morphological characterization of gastrointestinal tract toxicity was shown in the Supplementary Figure 2s, available at *Carcinogenesis* Online).

Sulindac inhibits pancreatic carcinogenesis in Pan$^{kras/p53}$ mice

The analysis of tumor development in the pancreas and metastasis to other organs was performed per our established protocols (31). For each mouse, the entire pancreas and surrounding small bowel were processed for a paraffin slide with hematoxylin and eosin stain (Figure 2A–C). No pancreatic tumors were identified in the wild-type mice (Figure 2A). An enlarged pancreas was observed in Pan$^{kras/p53}$ mice with extensive pancreatitis (Figure 2B) or large pancreatic tumor (Figure 2C), and massive pancreatic tumors were identified in all four Pan$^{kras/p53}$ mice in the AIN93M group with increased pancreas weights and two sulindac-treated Pan$^{kras/p53}$ mice with increased pancreas weights. Using established criteria in the literature (33), histopathological analysis was performed and showed that the pancreatic tumors were PDAC with either well, moderately (Figure 2D), or poorly differentiated patterns (Figure 2E). Ninety percent (18 of 20) of Pan$^{kras/p53}$ mice fed the regular AIN93M diet developed PDACs, whereas only 56% (9 of 16) of sulindac-treated Pan$^{kras/p53}$ mice developed PDACs (Figure 2G; X^2 = 5.4, P < 0.05). In the AIN93M group, of the tumor-bearing Pan$^{kras/p53}$ mice, 17% (3 of 18) of the PDACs were well to moderately differentiated and 83% were aggressive, poorly differentiated carcinomas. In contrast, in the sulindac-treated mice, 56% (5 of 9) of the PDACs were well to moderately well-differentiated and only 44% (4 of 9) were poorly differentiated (X^2 = 4.21, P < 0.05).

Metastasis of the PDACs was most commonly identified in the liver (Figure 2F) and occasionally in the lymph nodes. Metastatic PDAC was found in the liver in all four Pan$^{kras/p53}$ mice with increased liver weights. One of the Pan$^{kras/p53}$ mice with liver metastasis also showed metastasis to the lymph node. In the sulindac-treated group, only one Pan$^{kras/p53}$ mouse had lymph node metastasis and no liver metastasis was seen. Due to the limited number of mice with metastases, the difference in metastasis between Pan$^{kras/p53}$ mice and Pan$^{kras/p53}$ mice treated with sulindac did not reach statistical significance (Figure 2H, X^2 = 0.96, P > 0.05). Of note, high-grade lymphomas in the spleen (graded according to established criteria) (31) were observed in the three Pan$^{kras/p53}$ mice with increased spleen weights, whereas no lymphomas were observed in the sulindac-treated mice.

Sulindac inhibits Ki-67-labeled cell proliferation in Pan$^{kras/p53}$ mice but does not affect the expression levels of AKR1B10 and COX2

Ki-67-labeled cell proliferation was determined immunohistochemically. In Pan$^{kras/p53}$ mice fed the regular AIN93M diet, morphologically normal pancreatic acini showed occasional Ki-67 nuclear staining of proliferative cells (Figure 3A) and increased Ki-67 labeling was seen in acinar–ductal metaplasia in pancreatitis (Figure 3A), pancreatic intraepithelial neoplasia (PanIN lesions, Figure 3B) and PDAC (Figure 3C). In contrast, these lesions in sulindac-treated Pan$^{kras/p53}$ mice showed a marked decrease in cell proliferation (Figure 3D–F). In the Pan$^{kras/p53}$ mice without sulindac treatment, the proliferation index (percentage of Ki-67-positive cells in the total cells counted) was 56 ± 7.8% in PDACs, 30 ± 5.1% in PanIN lesions and 15 ± 3.3% in acinar–ductal metaplasia. A statistically significant reduction in Ki-67-labeled proliferation index was observed in these lesions in the sulindac-treatment mice (Figure 3G), and the proliferation index was 33 ± 7.2% in PDACs, 12 ± 2.3% in PanINs and 10 ± 2.3% in acinar–ductal metaplasia (Student's t-test, P < 0.01).

Because COX2 and AKR1B10 are the major targets of sulindac (a competitive inhibitor of these two enzymes), the expression status of COX2 and AKR1B10 were analyzed immunohistochemically in the pancreas of Pan$^{kras/p53}$ mice with or without sulindac administration. As seen in Figure 3H, the expression of COX2 was markedly increased in pancreatitis-PanINs lesion and PDAC compared with morphologically normal pancreatic parenchyma in Pan$^{kras/p53}$ mice without sulindac treatment. Similar expression levels of COX2 in pancreatitis-PanINs lesion and PDAC were observed in Pan$^{kras/p53}$ mice treated with sulindac as compared with the Pan$^{kras/p53}$ mice (Figure 3H) not given sulindac. Similar to COX2, the expression of AKR1B10 was markedly increased in pancreatitis-PanINs lesion and PDAC compared with morphologically normal pancreatic parenchyma in Pan$^{kras/p53}$ mice (Figure 3J) and a similar expression level of AKR1B10 in pancreatitis-PanINs lesion and PDAC was observed in Pan$^{kras/p53}$ mice treated with sulindac (Figure 3J). Histogram analysis in Photoshop further demonstrated that the immunostaining intensity of both COX2 (Figure 3I) and AKR1B10 (Figure 3K) were no significantly different in pancreatic lesions in Pan$^{kras/p53}$ mice treated with or without sulindac (Student's t-test, P > 0.05).

AKR1B10 activity and expression in mouse pancreatic carcinoma cells treated with sulindac in vitro

The P03 mouse pancreatic carcinoma cell line was derived from pancreatic PDACs in Pan$^{kras/p53}$ mice (C57B/6J background). P03 cells have been cultured *in vitro* for >2 years and >50 passages and have demonstrated their neoplastic features and epithelial origins with active mutant *Kras^{G12D}* and p53^{R172} genes (Supplementary Figure 3s, available at *Carcinogenesis* Online). Colony formation assays showed a dose-dependent inhibition of anchorage-independent growth or proliferation with IC_{50} 0.37 mM by sulindac.

To determine the effect of sulindac on AKR1B10 activity, oxidized reduced nicotinamide adenine dinucleotide phosphate was used as a monitor at 340 nm to measure AKR1B10 enzymatic activity in P03 pancreatic adenocarcinoma cell lysates treated with sulindac at doses of 0, 0.4, 0.8 and 1.6 μM (9). A significant inhibition of AKR1B10 enzymatic activity was observed at IC_{50} 0.7 μM (Figure 4A). Further, western blot assay revealed that the expression of AKR1B10 showed no change in P03 cells treated with sulindac compared with non-treated cells after normalization by β-actin (the protein loading control) (Figure 4B and C).

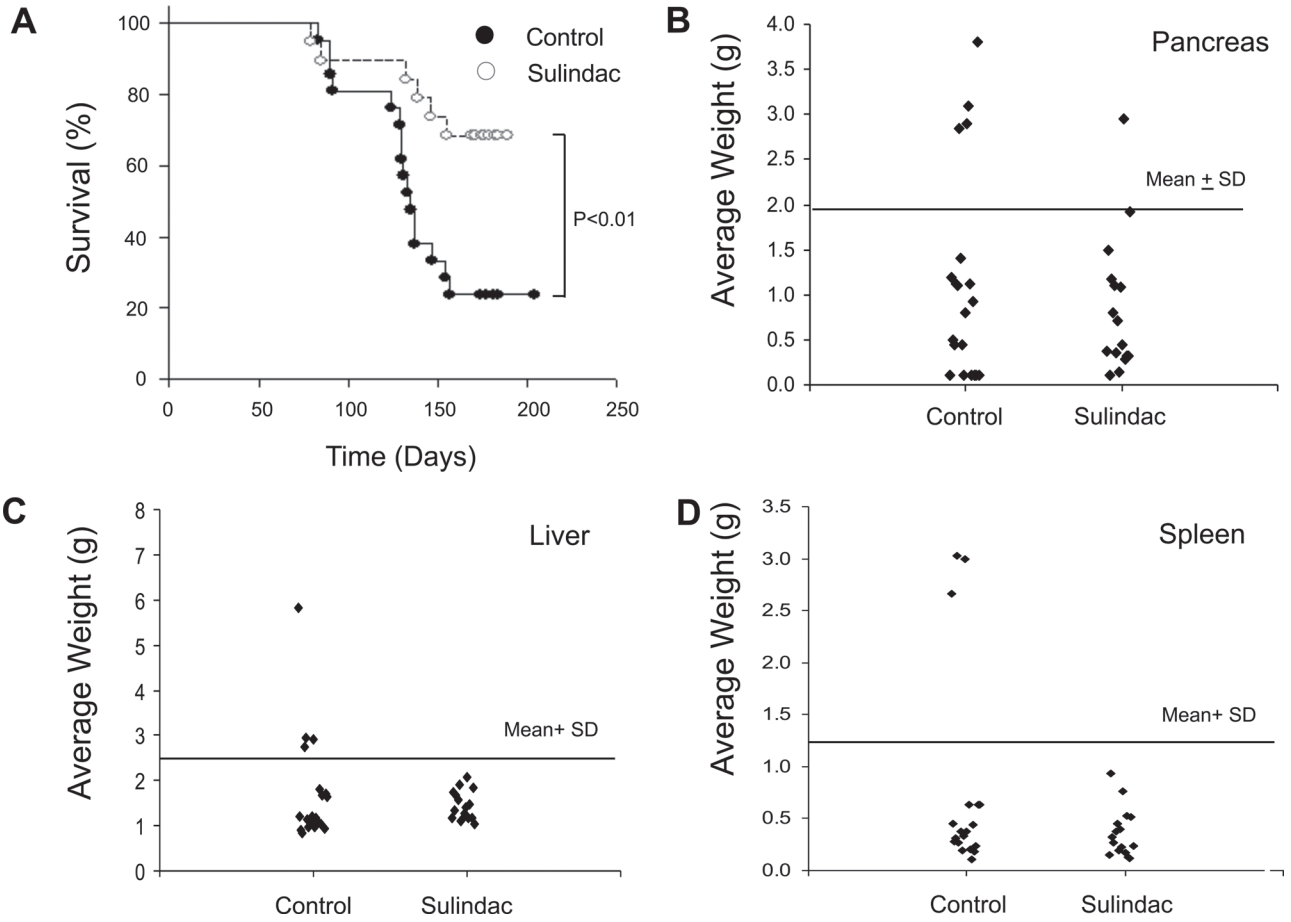

Fig. 1. Animal survival and key organ weights in Pan$^{kras/p53}$ mice. (**A**) Kaplan–Meier survival analysis: the log-rank statistic for the survival curves is greater than that would be expected by chance; there is a statistically significant difference between survival curves of Pan$^{kras/p53}$ mice fed diets with or without sulindac ($P < 0.01$). (**B–D**) Distribution of organ weights in Pan$^{kras/p53}$ mice fed diets with or without sulindac, including pancreas (B), liver (C) and spleen (D).

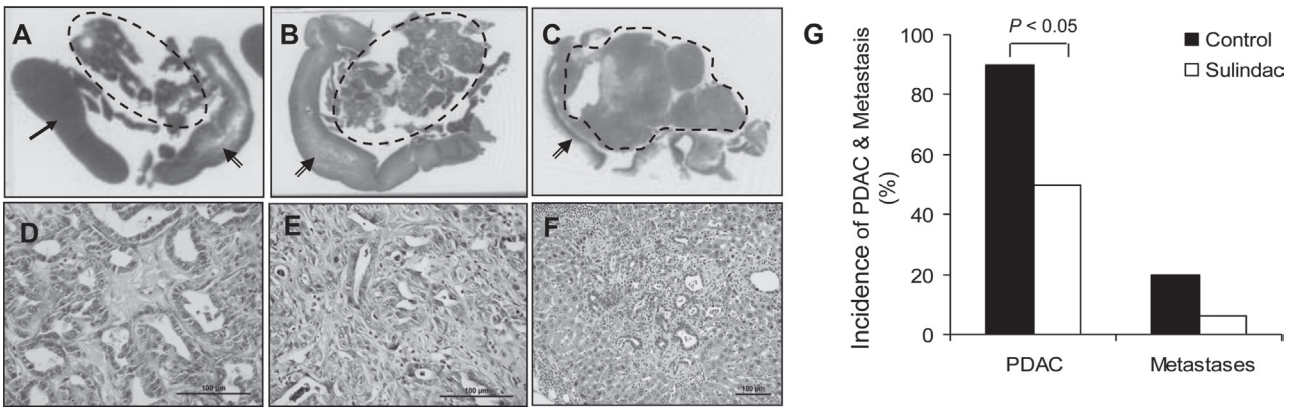

Fig. 2. Histopathological analysis of pancreatic tumors and metastasis. (**A–C**) Lower magnification of pancreas in the highlighted areas surrounded by duodenum (open arrow) and adjacent spleen (solid arrow), including pancreas from wild-type control mouse (A), enlarged pancreas with pancreatitis (B) or with pancreatic tumor (C) from Pan$^{kras/p53}$ mice. (**D–F**) High magnification of representative PDAC, includes a well-differentiated PDAC with glandular/tubular structure (D), moderately to poorly differentiated pancreatic ductal adenocarcinoma with sarcomatoid carcinoma feature and highly atypical nuclei (E) and metastatic PDAC in liver (F). (**G**) Histogram of the incidence of PDAC and its metastasis in Pan$^{kras/p53}$ mice treated with or without sulindac.

Inhibition of protein prenylation (Kras and human DNA-J homolog nuclear chaperone proteins) and Kras downstream signals in pancreatic carcinomas treated with sulindac in vitro and in vivo

Kras is an oncogenic protein that requires prenylation for its membrane localization and activity. Like other small guanosine triphosphatases, Kras regulates molecular events by cycling between an inactive guanosine diphosphate-bound form and an active guanosine triphosphate-bound form. The basis of its active state (guanosine triphosphate-bound) is a membrane-bound Kras protein or the prenylated form of the Kras protein. Detection of activated Kras protein and cell membrane-bound Kras serves as the best biomarker for determining protein prenylation status (31). Kras pull-down assay showed that the active form of Kras protein was significantly decreased in mouse P03 pancreatic carcinoma

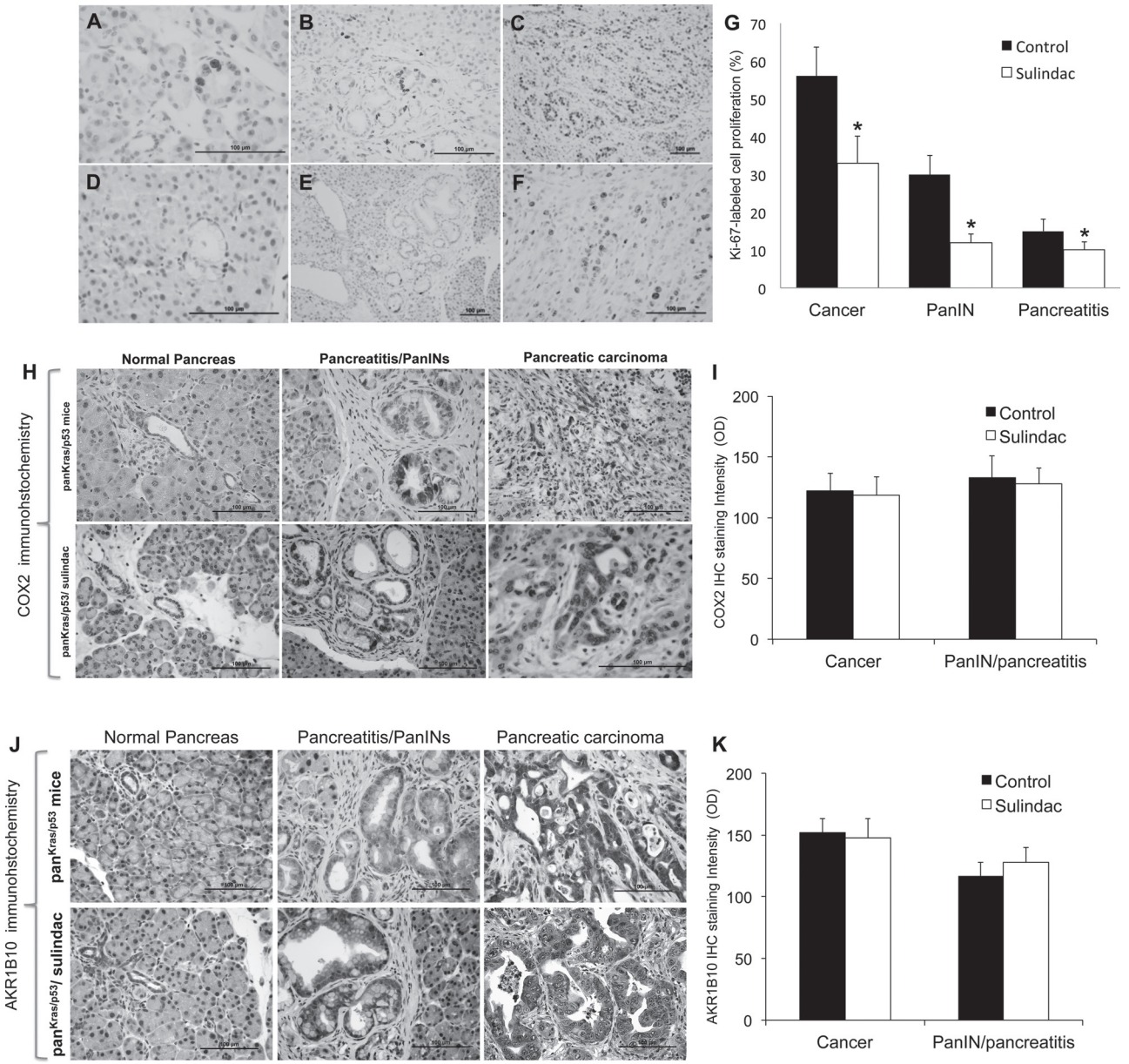

Fig. 3. Ki-67-labeled cell proliferation in pancreatic lesions in Pan$^{kras/p53}$ mice using an immunohistochemical approach. (**A–C**) Pancreatitis and acinar–ductal metaplasia (A), PanINs (B) and PDAC (C) in Pan$^{kras/p53}$ mice. (**D–F**) Pancreatitis and acinar–ductal metaplasia (D), PanINs (E) and PDAC (F) in Pan$^{kras/p53}$ mice treated with sulindac. (**G**) Histogram of Ki-67-labeled cell proliferation index in these pancreatic lesions in Pan$^{kras/p53}$ mice treated with or without sulindac (*statistical significance, $P < 0.01$). (**H**) Immunohistochemical analysis of COX2 expression in morphologically normal parenchyma, PanINs lesions and PDAC in Pan$^{kras/p53}$ mice treated with or without sulindac. (**I**) Histogram of COX2 immunostaining intensity in these pancreatic lesions in Pan$^{kras/p53}$ mice treated without or with sulindac (no statistical significance, $P > 0.05$). (**J**) Immunohistochemical analysis of AKR1B10 expression in morphologically normal parenchyma, PanINs lesions and PDAC in Pan$^{kras/p53}$ mice treated with or without sulindac. (**K**) Histogram of AKR1B10 immunostaining intensity in these pancreatic lesions in Pan$^{kras/p53}$ mice treated with or without sulindac (no statistical significance, $P > 0.05$).

cells treated with 0.4–1.6 mM sulindac as compared with total Kras protein (Figure 4B). In addition, membrane-bound Kras proteins were quantitatively analyzed using the western blot approach. Flotillin-2 membrane protein was used as a membrane protein loading control; for the extracted membrane proteins, western blotting showed a marked decrease in membrane-bound Kras protein in P03 cells treated with sulindac (Figure 4B). Human DNA-J homolog (HDJ2) protein, a co-chaperone containing a cysteine-rich zinc finger domain and a mitochondrial protein, is a heat-induced and farnesylated protein that is involved in mitochondrial protein import in mammals. HDJ2 is commonly used as another biomarker for the evaluation of protein prenylation (31). Sulindac-treated P03 cells showed a markedly increased level of non-farnesyled HDJ2 protein (Figure 4B). A quantitative densitometer analysis demonstrated that with 0.4–1.6 sulindac treatment, the active-form and membrane-bound prenylated Kras protein was significantly decreased and the non-farnesyled HDJ2 protein was significantly increased (histogram in Figure 4C; $P < 0.01$).

The effect of sulindac on the inhibition of Kras-mediated downstream signals, including phosphorylated c-raf, MEK1/2 and ERK1/2 proteins, was determined using the western blot approach with β-actin as a protein loading control. There was a marked decrease in all of these signals (Figure 4D). Quantitative densitometer analysis showed that with 0.4–1.6 sulindac treatment, Kras downstream-phosphorylated c-raf, MEK1/2 and ERK1/2 proteins were significantly reduced in P03 cells (histogram in Figure 4E, $P < 0.01$).

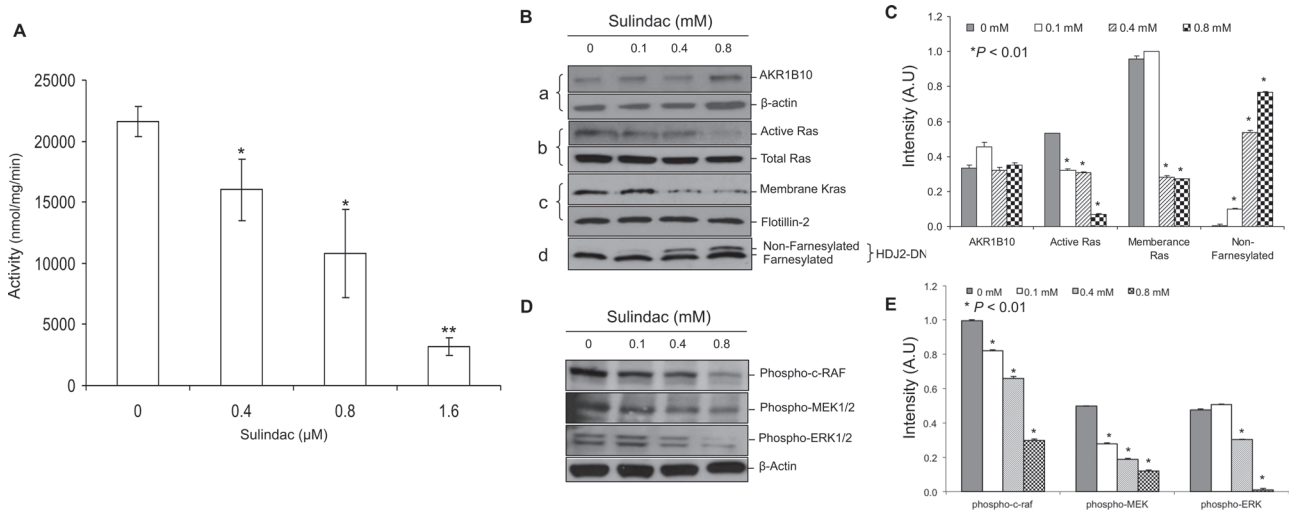

Fig. 4. Analysis of AKR1B10 enzyme activity, the active form and membrane-bound Kras protein and its downstream signals and prenylated HDJ2 proteins in mouse pancreatic carcinoma cell line P03. (**A**) Oxidized reduced nicotinamide adenine dinucleotide phosphate was used as a monitor at 340 nm for measuring AKR1B10 enzymatic activity and showed a dose-dependent inhibition of enzyme activity by sulindac. (**B**) Mouse P03 pancreatic carcinoma cells were treated with the indicated concentration of sulindac for 24 h and further analyzed with a western blot approach: from top down, western blot showed levels of AKR1B10 expression compared with β-actin, a protein loading control; active Ras Pull-down assay and western blot exhibited the levels of the active form Kras protein compared with total Kras protein; Western blot showed the levels of membrane-bound Kras protein compared with a Flotillin-2 membrane protein (membrane protein loading control) for the extracted membrane proteins as well as the levels of farnesylated and non-farnesylated HDJ2 protein. (**C**) Densitometry of the levels of protein expression was performed on the western blots. Values for AKR1B10, the active form or membrane-bound Kras, and HDJ2 proteins were normalized to the total loading control protein. (**D**) Mouse P03 pancreatic carcinoma cells treated with the indicated concentration of sulindac for 24 h were further analyzed with a western blot approach for Kras downstream signals including phosphorylated c-RAF, MEK1/2 and ERK1/2. (**E**) Densitometry of the levels of Kras downstream signals was performed on the western blots. The value for each protein was normalized to the total loading control protein. Statistically significant at $*P < 0.05$ and $**P < 0.01$.

To further determine the effect of AKR1B10 inhibition on modulating Kras-mediated downstream signals including c-Raf, MEK1/2 and Erk1/2, particularly phosphorylated ERK1/2 as a key mutant Kras-activated signal, immunohistochemical analysis for these signals was performed for the pancreas of Pan$^{kras/p53}$ mice treated with or without sulindac. Figure 5A shows the intense positive staining of phosphorylated ERK1/2 in acinar–ductal metaplasia in pancreatitis, PanINs and PDAC in Pan$^{kras/p53}$ mice receiving only the regular AIN93M diet. In sulindac-treated Pan$^{kras/p53}$ mice, only low-intensity staining of phosphorylated ERK1/2 was seen in these types of lesions (Figure 5B). Immunohistochemical staining intensity of phosphorylated ERK1/2 was quantitatively analyzed for at least 10 snapped images (under ×20 objective lens) of each lesion per pancreas (n = 3 mice/group). Histogram analysis in Photoshop showed that phosphorylated ERK1/2 was significantly decreased in pancreatic lesions in sulindac-treated Pan$^{kras/p53}$ mice (Figure 5C, Student's t-test, $P < 0.05$). Other mutant Kras-activated signals including phosphorylated c-Raf and MEK1/2 were further analyzed immunohistochemically. The results showed intense positive staining of phosphorylated c-Raf (Figure 5D) and phosphorylated MEK1/2 (Figure 5F) in PanINs and PDAC in Pan$^{kras/p53}$ mice receiving only the regular AIN93M diet. In sulindac-treated Pan$^{kras/p53}$ mice, only low-intensity staining of phosphorylated c-Raf (Figure 5D) and phosphorylated MEK1/2 (Figure 5F) was seen in these types of lesions. Histogram analysis in Photoshop further demonstrated that the immunostaining intensity of both phosphorylated c-Raf (Figure 5E) and phosphorylated MEK1/2 (Figure 5G) were significantly different in pancreatic PanINs and PDAC in Pan$^{kras/p53}$ mice compared with Pan$^{kras/p53}$ mice treated with sulindac (Student's t-test, $P < 0.05$).

siRNA silencing of AKR1B10 results in inhibition of Kras activation and its downstream signal

To further confirm the effects of sulindac treatment on inhibiting AKR1B10 and its modulated protein prenylation, silencing of AKR1B10 dynamic expression in the P03 pancreatic adenocarcinoma cell line was achieved using a siRNA approach. As seen in Figure 6A, P03 pancreatic carcinoma cells transfected with siRNA showed significantly lower AKR1B10 enzyme activity as compared with scrambled RNA. Western blot assay further confirmed that AKR1B10 expression was significantly lower as compared with the scrambled siRNA control P03 cell line with β-actin as a protein loading control (Figure 6B, upper graph).

P03 cells with siRNA silencing of AKR1B10 expression showed a significant decrease in active form Kras protein as detected using Kras pull-down assay (Figure 6B). Kras downstream signals were also evaluated and showed that the phosphorylation of ERK1/2 and MEK1/2 was markedly downregulated in P03 cells with AKR1B10 silencing (Figure 6B). To determine whether AKR1B10 is involved in the process of protein prenylation, farnesylated and non-farnesylated HDJ2 proteins were analyzed using a western blot approach and showed that an increased level of non-farnesyled HDJ2 protein was observed in siRNA AKR1B10 silenced cells as compared with scrambled siRNA control cells (Figure 6B, upper band). Quantitative densitometer analysis demonstrated that AKR-1B10, the active form of Kras and Kras downstream phosphorylated-MEK1/2 and ERK1/2 proteins were significantly reduced, and non-farnesylated HDJ2 protein was significantly increased in P03 cells with siRNA-silencing AKR1B10 (histogram in Figure 6C, $P < 0.05$).

Discussion

Pancreatic cancer is one of the most lethal malignancies, and chronic pancreatitis is a well-known risk factor for the development of pancreatic carcinomas. Multiple genetic alterations including *kras* and *p53* gene mutations have been identified in pancreatic carcinogenesis (36). The reproducibility of pancreatic carcinogenesis in Pan$^{kras/p53}$ mice allows us to explore the chemopreventive effect of sulindac on the development of pancreatic cancer and other molecular target/s (31). NSAIDs such as sulindac are the most commonly used drugs for inflammation and pain worldwide and intriguingly, studies have also shown that NSAIDs and coxibs are the most promising

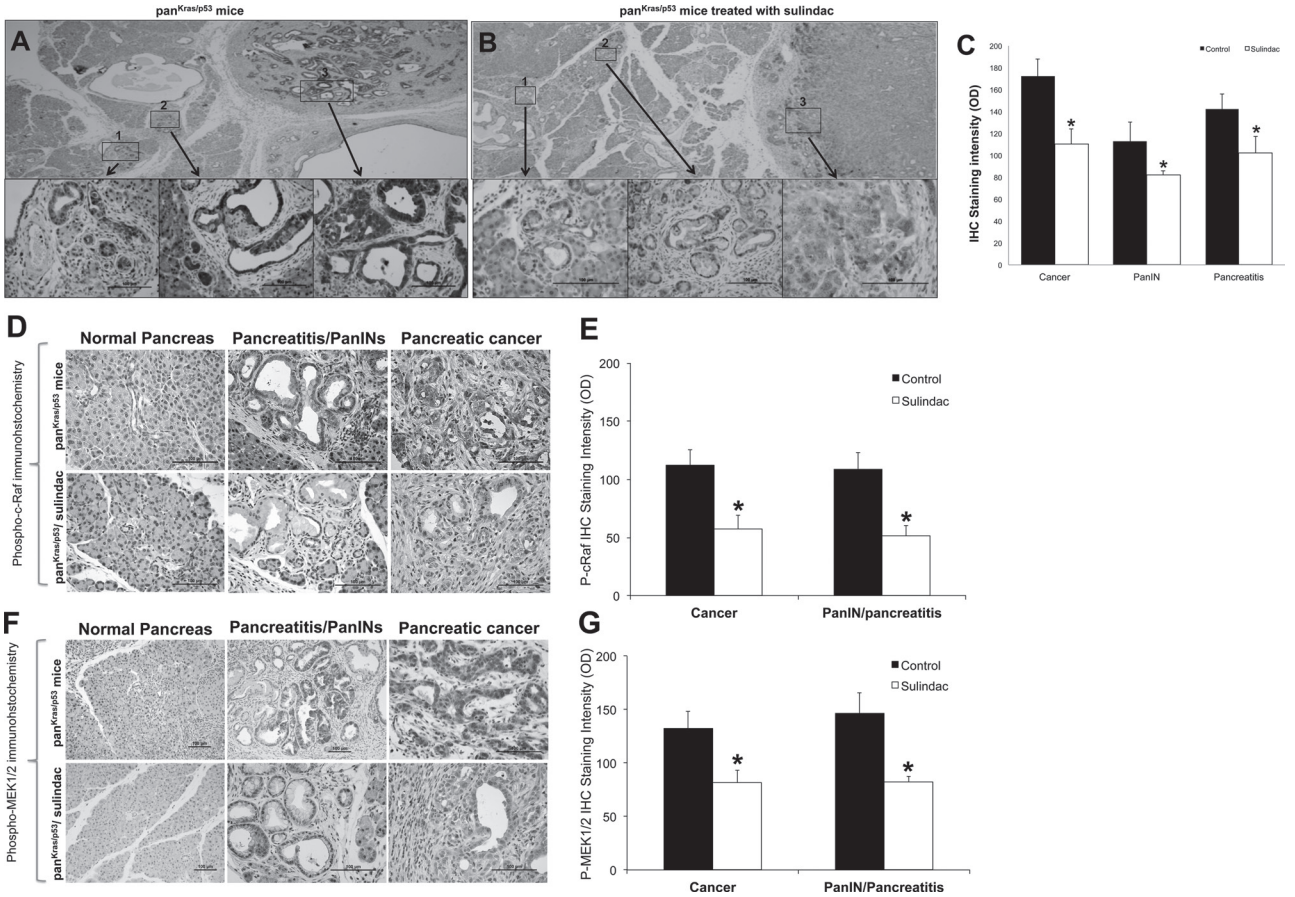

Fig. 5. Immunohistochemical analysis of phosphorylated ERK1/2 protein. (**A**) Pancreas of Pan$^{kras/p53}$ mice and square areas were further magnified for the lesions of pancreatitis, PanINs and PDAC. (**B**) Pancreas of Pan$^{kras/p53}$ mice treated with sulindac; square areas were further magnified for the lesions of pancreatitis, PanINs and PDAC. (**C**) Histogram of staining intensity of phosphorylated ERK1/2 in PDAC, PanINs and pancreatitis in Pan$^{kras/p53}$ mice treated with or without sulindac (*statistically significant, $P < 0.05$). (**D**) Phosphorylated c-Raf immunohistochemistry for morphologically normal pancreas, pancreatitis/PanINs and PDAC in Pan$^{kras/p53}$ mice treated with or without sulindac. (**E**) Histogram of staining intensity of phosphorylated c-Raf in PDAC and PanINs/pancreatitis in Pan$^{kras/p53}$ mice treated with or without sulindac (*statistically significant, $P < 0.05$). (**F**) Phosphorylated MEK1/2 immunohistochemistry for morphologically normal pancreas, pancreatitis/PanINs and PDAC in Pan$^{kras/p53}$ mice treated with or without sulindac. (**G**) Histogram of staining intensity of phosphorylated MEK1/2 in PDAC and PanINs/pancreatitis in Pan$^{kras/p53}$ mice treated with or without sulindac (*statistically significant, $P < 0.05$).

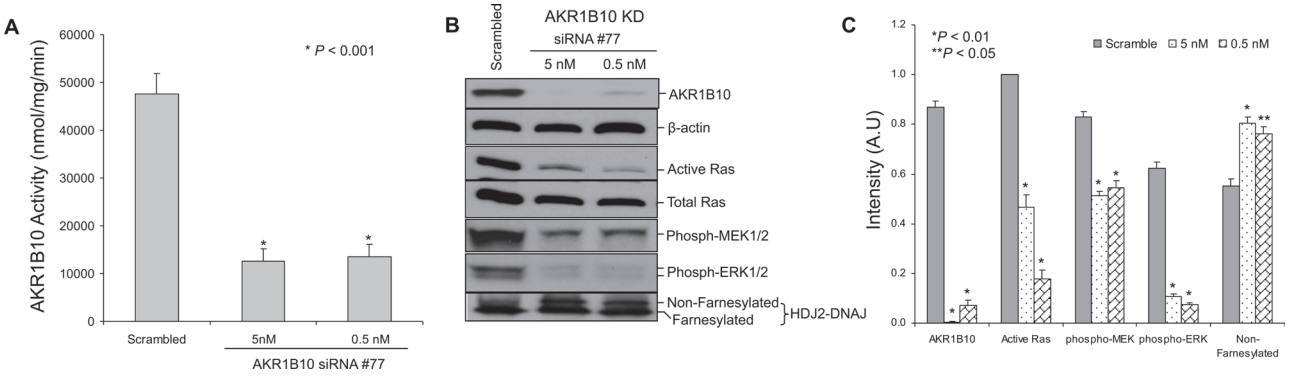

Fig. 6. siRNA-mediated silencing of AKR1B10 expression and enzymatic activity resulted in the reduction of prenylated Kras and HDJ2 proteins and suppression of Kras downstream signals. (**A**) AKR1B10 enzymatic activity. (**B**) Western blot analysis for AKR1B10, the active form Kras, phosphorylated MEK1/2 and ERK1/2 and HDJ2 proteins. (**C**) Densitometry of the expression levels of AKR1B10, the active form Kras and its downstream signals, and HDJ2 proteins were performed on the western blots. The value for each protein was normalized to the total loading control protein.

agents in development today for the cancer chemoprevention (5,37). We are the first to report on the significant chemopreventive effects of sulindac on pancreatic carcinogenesis in Pan$^{kras/p53}$ mice and to show that the use of sulindac led to significant increases in animal survival from pancreatic carcinoma development and decreases in pancreatic cancer incidence and metastasis.

To rule out the effects of sulindac on Pdx-cre, the activation of transgenic mutant *Kras*^{G12D} and *p53*^{R172H} genes by Pdx-1-cre recombination was analyzed in pancreatic tumors using specific PCR and p53 immunohistochemistry approaches. There were no differences in the recombinant *Kras*^{G12D} and *p53*^{R172H} genes in pancreatic tumors, and p53 immunostaining revealed an accumulation of mutant p53

protein in early acinar–ductal metaplasia, PanINs and PDAC in Pan$^{kras/p53}$ mice fed either AIN93M diet or diet containing 200 p.p.m. sulindac (Supplementary Figure 4s, available at *Carcinogenesis* Online).

One crucial question in our experiments was whether the 200 p.p.m. dose of sulindac could be comparable with the human dosage. In general, animal doses cannot be extrapolated to a human equivalent dose by simple conversion based on body weight due to significant differences in multiple aspects, including metabolic rates (26). The most appropriate conversion tool for comparison of drug doses from animal studies (specifically rodents) to humans is the bovine serum albumin normalization method, as recommended by the Food and Drug Administration (32). To find the human equivalent dose, the formula human equivalent dose (mg/kg) = animal dose (mg/kg) × animal Km/hum Km (the animal Km is 3 in mice and the human Km is 37) is used. In humans, the safe long-term dose of sulindac as an analgesic and anti-inflammatory is 400 mg daily (200 mg, twice per day). In a hypothetical 75 kg patient, a 400 mg/day dose works out to be 5.3 mg/kg. Using that per kilogram dose, the equivalent animal dose would be 65.8 mg/kg per mouse per day with a daily total dose of 1.65 mg in an average 25 g mouse. Further translating this dose into an actual diet concentration: the average mouse consumes 2 g (0.002 kg) of food per day, and the concentration of the sulindac in the diet should be 1.65 mg/0.002 kg food. This would be equal to 823 mg sulindac/kg food, which is equal to 823 p.p.m. of sulindac in the mouse diet. Our mice were only receiving sulindac doses of 200 p.p.m., four times below the 823 p.p.m. 'maximum' dose of sulindac based on human clinical dosage guidelines.

Sulindac is a NSAID of the indene acetic acid class. The absorption of sulindac is rapid when given orally. Based on Food and Drug Administration pharmacokinetic data, sulindac and its sulfone and sulfide metabolites are predominantly bound to plasma albumin after absorption. Plasma protein binding measured over a concentration range was constant (0.5–2.0 μg/ml). Biochemical and pharmacological evidence indicates that the activity of sulindac resides in its sulfide metabolite for COX2 inhibition. But, the active sulfide metabolite only accounts for <6% of the total intestinal exposure to sulindac and its metabolites. Recirculation of the parent drug sulindac and its sulfone metabolite is more extensive than that of the active sulfide metabolite. Whether or not the parent drug sulindac and its sulfone metabolite have anticancer activity beyond COX2 inhibition is not well known. AKR1B10 has been implicated as a molecular target of sulindac (8). Upregulation of AKR1B10 in pancreatic cancer and other malignant cancer has been identified (9). In this study, we have further demonstrated that AKR1B10 is overexpressed in murine pancreatic carcinoma cells *in vitro* and *in vivo* and that sulindac inhibited AKR1B10 enzyme activity with IC_{50} 0.7 μM in these cells.

It has been proposed that AKR1B10 is involved in the process of protein prenylation by metabolizing isoprenoids or recycling intracellular farnesal/geranylgeranial (9,38). Labeling the substrates of prenyltransferase, farnesyl and geranylgeranyl pyrophosphates, with either biotin or radioisotopes would be a key step in designing an efficient assay for detecting/profiling prenylated proteins by considering the sole source of farnesyl and geranylgeranyl pyrophosphates from the mevalonate pathway or for detecting the effect of a prenyltransferase inhibitor. However, intracellular farnesal/geranylgeranial can be reduced by AKR1B10 and further phosphorylated into farnesyl and geranylgeranyl pyrophosphates, which would serve as another source of substrates for protein prenylation. Thus, the assays labeling farnesyl and geranylgeranyl pyrophosphates would be not accurate or efficient in detecting protein prenylation via targeting AKR1B10. Therefore, prenylated proteins including Kras and human DNA-J homolog (HDJ2) chaperone are crucial prototypical biomarkers for detecting the effect of AKR1B10 inhibition on protein prenylation. In this study, we have first demonstrated that the active form or membrane-bound prenylated Kras protein is significantly decreased in murine pancreatic carcinoma cells treated with sulindac; and in the parallel, a significant increase in non-prenylated form HDJ2 protein is also found. siRNA silencing of AKR1B10 expression in these murine pancreatic carcinoma cells resulted in similar results as sulindac treatment—a significant decrease in active form/membrane-bound prenylated Kras protein and a significant increase in non-prenylated form HDJ2 protein. These results indicate that AKR1B10 is involved in the process of protein prenylation.

Kras mutation is the most common early genetic alteration in pancreatic cancer, and the activation of mutant Kras protein requires prenylation for its membranous localization/activity. Obviously, the next question would be whether targeting Kras protein prenylation by sulindac affects Kras activity in mutant *Kras*-initiated pancreatic carcinogenesis in Pan$^{kras/p53}$ mice. In sulindac-treated Pan$^{kras/p53}$ mice, we demonstrated that Ki-67-labeled cell proliferation and phosphorylated ERK1/2 (downstream of Kras gene) were both significantly decreased in PanIN lesions and pancreatic carcinomas. We further identified that murine pancreatic carcinoma cells P03 either treated with sulindac or with AKR1B10 silenced by siRNA showed significant reductions in the Kras downstream-phosphorylated c-raf, MEK1/2 and ERK1/2 proteins. These results indicate that the inhibition or knockdown of AKR1B10 resulted in the suppression of Kras protein prenylation and Kras downstream signaling activities, leading to the inhibition of pancreatic carcinogenesis.

In addition to metabolizing lipids/isoprenoids, AKR1B10 is involved in metabolizing active carbonyls and in regulating retinal homeostasis. For carbonyl metabolism in AKR1B10-overexpressed neoplastic cells, the conversion of highly reactive aldehyde and ketone groups into hydroxyl groups by AKR1B10 prevents the cell from undergoing carbonyl-induced apoptosis. There are numerous reports indicating that the sulindac is a strong apoptosis inducer probably by inhibiting AKR1B10. AKR1B10 is also an efficient retinal reductase; the conversion of retinal to retinol by AKR1B10 results in the suppression of retinal to retinoic acid conversion, which is important because retinoic acid is a major active antineoplastic metabolite. Additional study is needed to further address the role of these metabolic fates in carcinogenesis.

In summary, we have demonstrated that sulindac is a strong agent for inhibiting pancreatic carcinogenesis in Pan$^{kras/p53}$ mice. Mechanistically, the inhibition of AKR1B10 by sulindac is paralleled with siRNA silencing of AKR1B10 expression, showing a significant decrease in Kras and HDJ2 protein prenylation, and inhibition of KRAS downstream effectors. Taken together, these findings strongly suggest that sulindac has extremely high potential as a chemopreventive agent for pancreatic cancer and targeting of AKR1B10 by sulindac appears to be one of the key mechanisms for the inhibition of protein prenylation and carcinogenesis.

Supplementary material

Supplementary Figures 1–4 can be found at http://carcin.oxfordjournals.org/

Funding

National Institutes of Health R01 grant (CA164041).

Conflict of Interest Statement: None declared.

References

1. Koornstra,J.J. *et al.* (2005) Sulindac inhibits beta-catenin expression in normal-appearing colon of hereditary nonpolyposis colorectal cancer and familial adenomatous polyposis patients. *Cancer Epidemiol. Biomarkers Prev.*, **14**, 1608–1612.
2. Rao,C.V. *et al.* (1995) Chemoprevention of colon carcinogenesis by sulindac, a nonsteroidal anti-inflammatory agent. *Cancer Res.*, **55**, 1464–1472.
3. Reddy,B.S. *et al.* (1999) Chemopreventive efficacy of sulindac sulfone against colon cancer depends on time of administration during carcinogenic process. *Cancer Res.*, **59**, 3387–3391.
4. Rijcken,F.E. *et al.* (2007) Sulindac treatment in hereditary non-polyposis colorectal cancer. *Eur. J. Cancer*, **43**, 1251–1256.

5. Cuzick,J. *et al.* (2009) Aspirin and non-steroidal anti-inflammatory drugs for cancer prevention: an international consensus statement. *Lancet Oncol*., **10**, 501–507.
6. Piazza,G.A. *et al.* (1995) Antineoplastic drugs sulindac sulfide and sulfone inhibit cell growth by inducing apoptosis. *Cancer Res*., **55**, 3110–3116.
7. Tegeder,I. *et al.* (2001) Cyclooxygenase-independent actions of cyclooxygenase inhibitors. *FASEB J*., **15**, 2057–2072.
8. Stanger,B.Z. *et al.* (2005) Pten constrains centroacinar cell expansion and malignant transformation in the pancreas. *Cancer Cell*, **8**, 185–195.
9. Chung,Y.T. *et al.* (2012) Overexpression and oncogenic function of aldo-keto reductase family 1B10 (AKR1B10) in pancreatic carcinoma. *Mod. Pathol*., **25**, 758–766.
10. Heringlake,S. *et al.* (2010) Identification and expression analysis of the aldo-ketoreductase1-B10 gene in primary malignant liver tumours. *J. Hepatol*., **52**, 220–227.
11. Cao,D. *et al.* (1998) Identification and characterization of a novel human aldose reductase-like gene. *J. Biol. Chem*., **273**, 11429–11435.
12. Cao,D. *et al.* (2004) Identification of novel highly expressed genes in pancreatic ductal adenocarcinomas through a bioinformatics analysis of expressed sequence tags. *Cancer Biol. Ther*., **3**, 1081–1089; discussion 1090.
13. Fukumoto,S. *et al.* (2005) Overexpression of the aldo-keto reductase family protein AKR1B10 is highly correlated with smokers' non-small cell lung carcinomas. *Clin. Cancer Res*., **11**, 1776–1785.
14. Kim,J.L. *et al.* (2007) Overexpression of HMG-CoA reductase, a potential therapeutic target for pancreatic adenocarcinoma. *Mod. Pathol.*, **20**(Suppl. 2), 284A.
15. Penning,T.M. (2005) AKR1B10: a new diagnostic marker of non-small cell lung carcinoma in smokers. *Clin. Cancer Res*., **11**, 1687–1690.
16. Qiu,W. *et al.* (2010) Chemoprevention by nonsteroidal anti-inflammatory drugs eliminates oncogenic intestinal stem cells via SMAC-dependent apoptosis. *Proc. Natl Acad. Sci. USA*, **107**, 20027–20032.
17. Woenckhaus,M. *et al.* (2006) Smoking and cancer-related gene expression in bronchial epithelium and non-small-cell lung cancers. *J. Pathol*., **210**, 192–204.
18. Su,A.I. *et al.* (2004) A gene atlas of the mouse and human protein-encoding transcriptomes. *Proc. Natl Acad. Sci. USA*, **101**, 6062–6067.
19. Guerra,C. *et al.* (2007) Chronic pancreatitis is essential for induction of pancreatic ductal adenocarcinoma by K-Ras oncogenes in adult mice. *Cancer Cell*, **11**, 291–302.
20. Ciolino,H.P. *et al.* (2008) Sulindac and its metabolites induce carcinogen metabolizing enzymes in human colon cancer cells. *Int. J. Cancer*, **122**, 990–998.
21. Martin,H.J. *et al.* (2009) Role of human aldo-keto-reductase AKR1B10 in the protection against toxic aldehydes. *Chem. Biol. Interact*., **178**, 145–150.
22. Quinn,A.M. *et al.* (2008) Oxidation of PAH trans-dihydrodiols by human aldo-keto reductase AKR1B10. *Chem. Res. Toxicol*., **21**, 2207–2215.
23. Gao,J. *et al.* (2009) CAAX-box protein, prenylation process and carcinogenesis. *Am. J. Transl. Res*., **1**, 312–325.
24. Youssef,S. *et al.* (2002) The HMG-CoA reductase inhibitor, atorvastatin, promotes a Th2 bias and reverses paralysis in central nervous system autoimmune disease. *Nature*, **420**, 78–84.
25. Crosas,B. *et al.* (2003) Human aldose reductase and human small intestine aldose reductase are efficient retinal reductases: consequences for retinoid metabolism. *Biochem. J*., **373**(Pt 3), 973–979.
26. Grippo,P.J. *et al.* (2005) Modeling pancreatic cancer in animals to address specific hypotheses. *Methods Mol. Med*., **103**, 217–243.
27. Leach,S.D. (2004) Mouse models of pancreatic cancer: the fur is finally flying! *Cancer Cell*, **5**, 7–11.
28. Jackson,E.L. *et al.* (2001) Analysis of lung tumor initiation and progression using conditional expression of oncogenic K-ras. *Genes Dev*., **15**, 3243–3248.
29. Johnson,L. *et al.* (2001) Somatic activation of the K-ras oncogene causes early onset lung cancer in mice. *Nature*, **410**, 1111–1116.
30. Hingorani,S.R. *et al.* (2005) Trp53R172H and KrasG12D cooperate to promote chromosomal instability and widely metastatic pancreatic ductal adenocarcinoma in mice. *Cancer Cell*, **7**, 469–483.
31. Liao,J. *et al.* (2012) Atorvastatin inhibits pancreatic carcinogenesis and increases survival in LSL-Kras(G12D)-LSL-Trp53(R172H)-Pdx1-Cre mice. *Mol Carcinog*., [Epub ahead of print].
32. Reagan-Shaw,S. *et al.* (2008) Dose translation from animal to human studies revisited. *FASEB J*., **22**, 659–661.
33. Hruban,R.H. *et al.* (2006) Pathology of genetically engineered mouse models of pancreatic exocrine cancer: consensus report and recommendations. *Cancer Res*., **66**, 95–106.
34. Bai,H. *et al.* (2011) Inhibition of chronic pancreatitis and pancreatic intraepithelial neoplasia (PanIN) by capsaicin in LSL-KrasG12D/Pdx1-Cre mice. *Carcinogenesis*, **32**, 1689–1696.
35. Seril,D.N. *et al.* (2002) Inhibition of chronic ulcerative colitis-associated colorectal adenocarcinoma development in a murine model by N-acetylcysteine. *Carcinogenesis*, **23**, 993–1001.
36. Duell,E.J. (2012) Epidemiology and potential mechanisms of tobacco smoking and heavy alcohol consumption in pancreatic cancer. *Mol. Carcinog*., **51**, 40–52.
37. Fischer,S.M. *et al.* (2011) Coxibs and other nonsteroidal anti-inflammatory drugs in animal models of cancer chemoprevention. *Cancer Prev. Res. (Phila)*., **4**, 1728–1735.
38. Endo,S. *et al.* (2011) Roles of rat and human aldo-keto reductases in metabolism of farnesol and geranylgeraniol. *Chem. Biol. Interact*., **191**, 261–268.

Received December 10, 2012; revised May 9, 2013; accepted May 13, 2013